

Introduction

White emitting pcLEDs based on a blue emitting LED and a yellow emitting phosphor, for example YAG:Ce³⁺, are commonly used as solid state light sources for general lighting. However, such systems suffer from rather low color rendering and luminous efficacy, due to missing radiation in the green and deep red spectral range. In addition to that, the color point of the chip/converter stack depends strongly on the thickness of the phosphor layer located on the LED-chip. On this scale it is a manufacturing challenge to maintain constant layer thickness and therefore stability of color points. Another approach to obtain white light is the conversion of UV radiation by a white emitting phosphor. In this approach the color point depends only on the phosphor blend. One possibility to generate a white emitting phosphor is the incorporation of Ce³⁺ and Mn²⁺ in a host structure. The broad emissions bands in the blue and red spectral region of Ce³⁺ and Mn²⁺ yield white light due to additive color mixing. Since the emitting transitions in Mn²⁺ are spin- and parity-forbidden, it has to be sensitized by energy transfer from Ce³⁺ to Mn²⁺.

To synthesize a new white emitting phosphor samples, of monoclinic Ca₃Y₂(Si₃O₉)₂ doped with Ce³⁺ and Mn²⁺ were prepared and its luminescent properties were investigated.

Table 1
Crystal structure data of Ca₃Y₂(Si₃O₉)₂ (Data from Endo et al., Acta Crystallogr. C 1997, C53, 1533–1536).

Ca ₃ Y ₂ (Si ₃ O ₉) ₂	
Crystal system	monoclinic
Space group	C ₂ /c
Cell parameters	a = 13.320 Å b = 7.729 Å c = 14.785 Å β = 90.256°

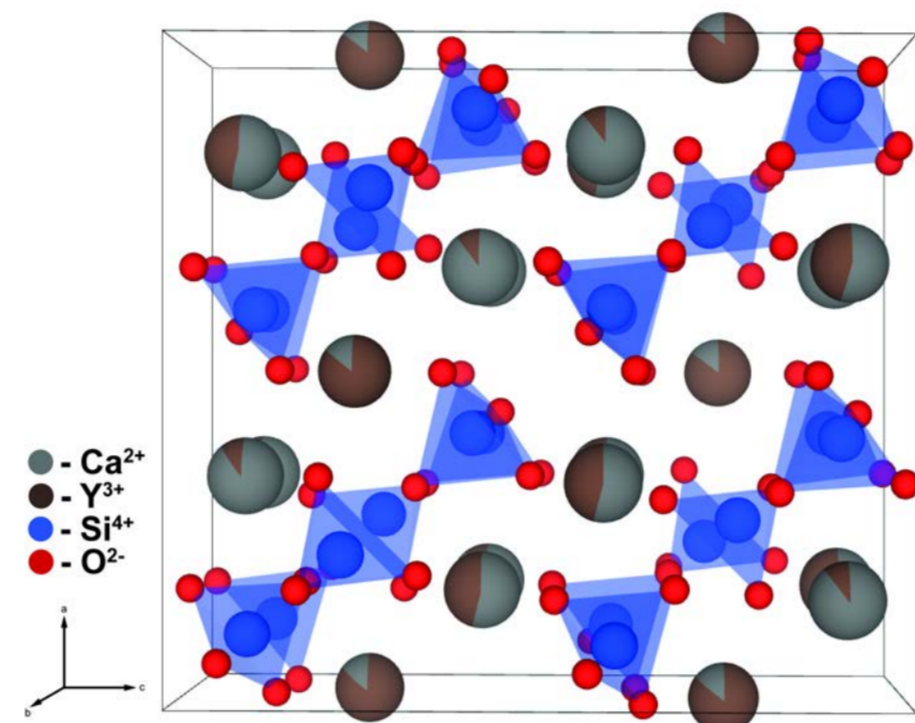


Fig. 1. Unit cell of Ca₃Y₂(Si₃O₉)₂ (Drawn with VESTA, K. Momma, F. Izumi, J. Appl. Crystallogr. 2011, 44, 1272-1276).

Experimental Section

The phosphor samples were synthesized by conventional solid state synthesis. The high purity starting materials CaCO₃ (Ph. Eur., Dr. Paul Lohmann), Y₂O₃ (99.99%, Treibacher), SiO₂ (99.0%, Merck), CeO₂ (99.9%, Atomergic Chemicals Co.) and MnC₂O₄·2H₂O (chem. Pure, Dr. Paul Lohmann) were grinded in an agate mortar in Acetone and transferred subsequently into an alumina crucible. The samples were calcinated between 1200 and 1400 °C for 8 h in a reductive CO atmosphere.

Phase purity was investigated by application of powder X-ray diffraction. Therefore the diffractometer Miniflex II from Rigaku with Bragg-Brentano geometry was used. Optical properties of the phosphors were characterized by recording excitation and emission spectra as well as reflectance spectra. Furthermore decay times of the phosphors were measured. Excitation and emission spectra were recorded with a fluorescence spectrometer from Edinburgh Instruments Ltd (FLS920) equipped with 450 W Xe lamp. For reflectance measurements the spectrometer was additionally equipped with an Ulbricht sphere coated with BaSO₄. Decay time measurements were performed using a picosecond pulsed laser.

Results

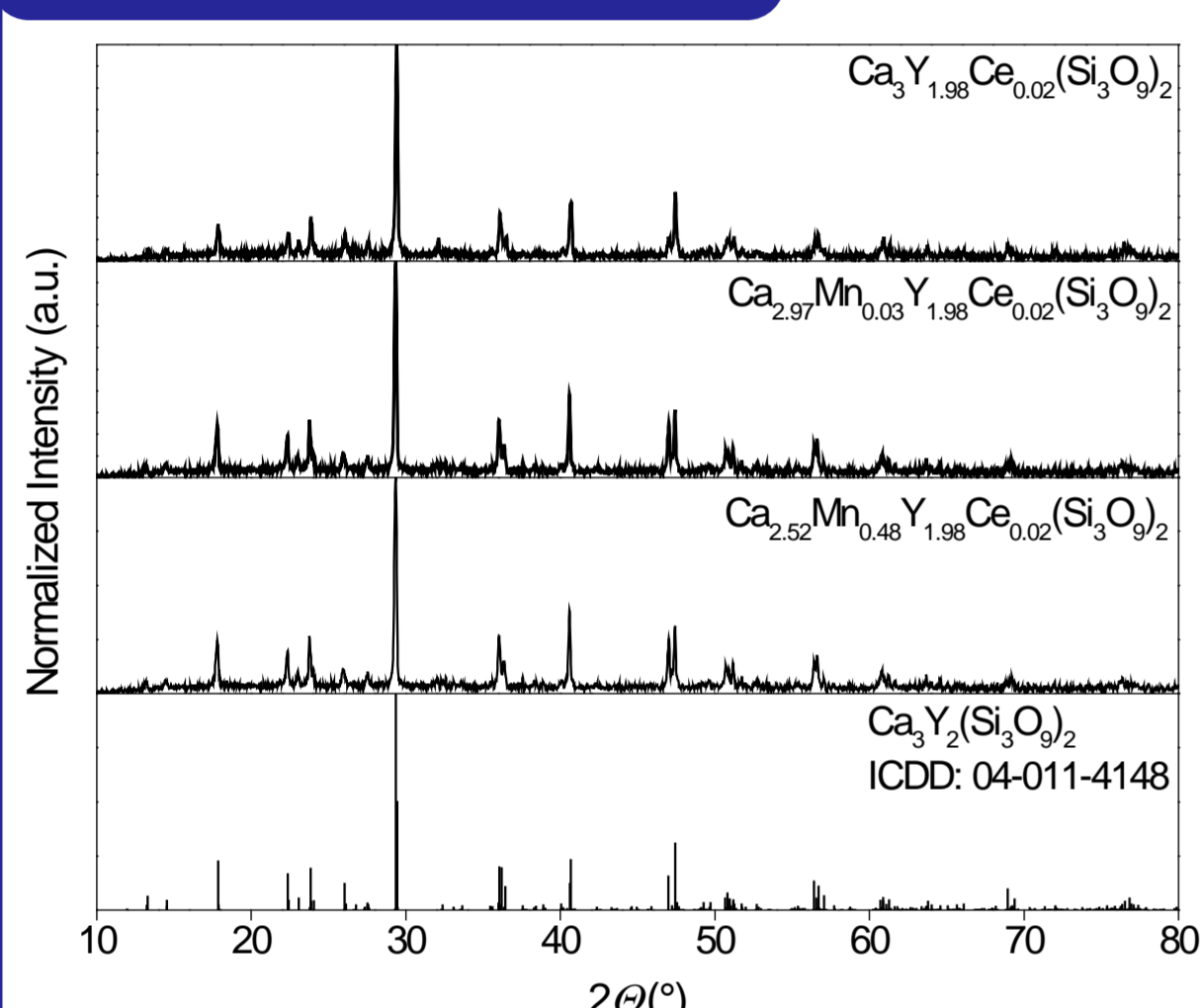


Fig. 2. Randomly selected X-ray diffraction patterns of Ca₃Y₂(Si₃O₉)₂:Ce³⁺,Mn²⁺ as well as the ICDD reference card of Ca₃Y₂(Si₃O₉)₂.

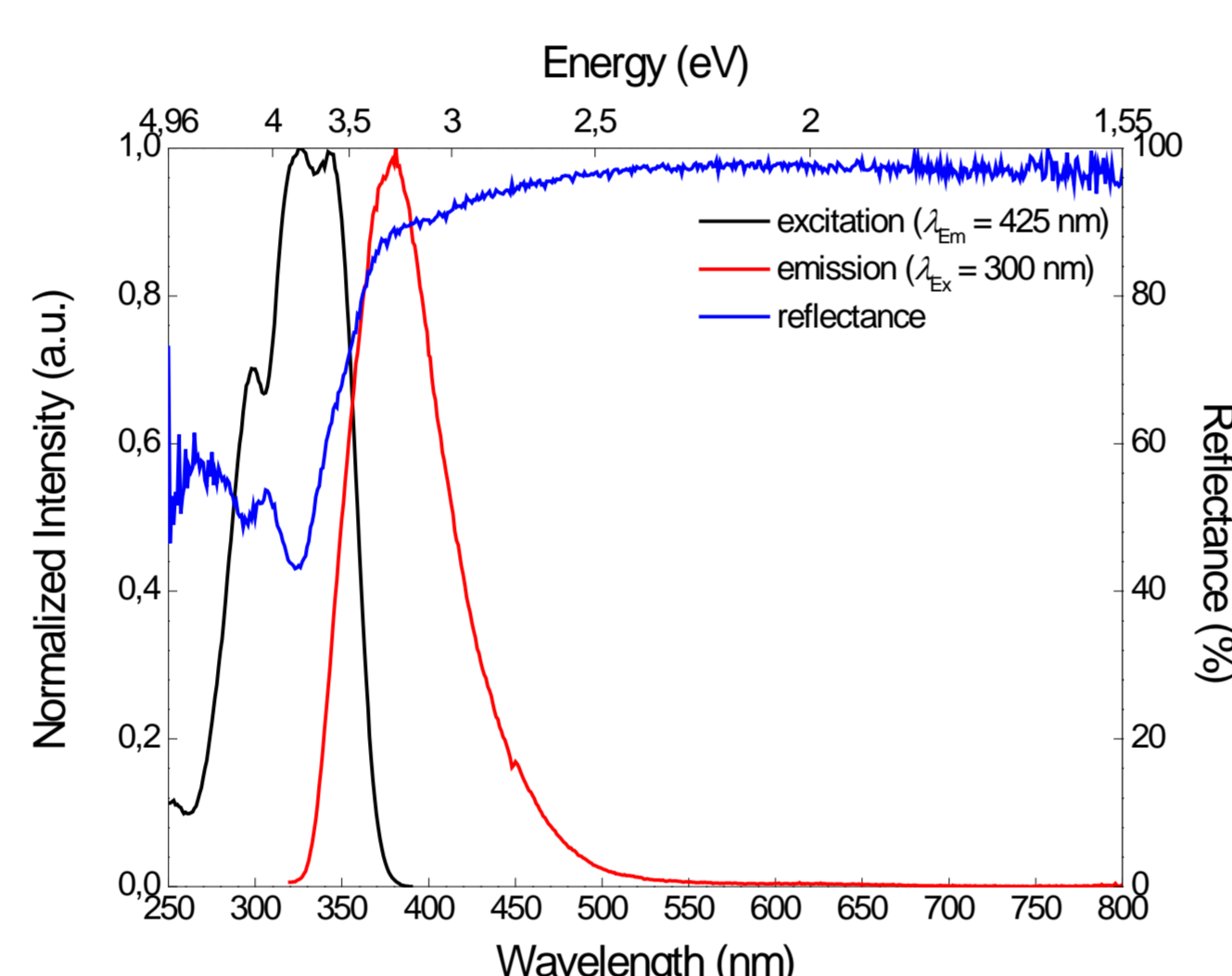


Fig. 3. Excitation, emission and reflectance spectra of Ca₃Y_{1.98}Ce_{0.02}(Si₃O₉)₂.

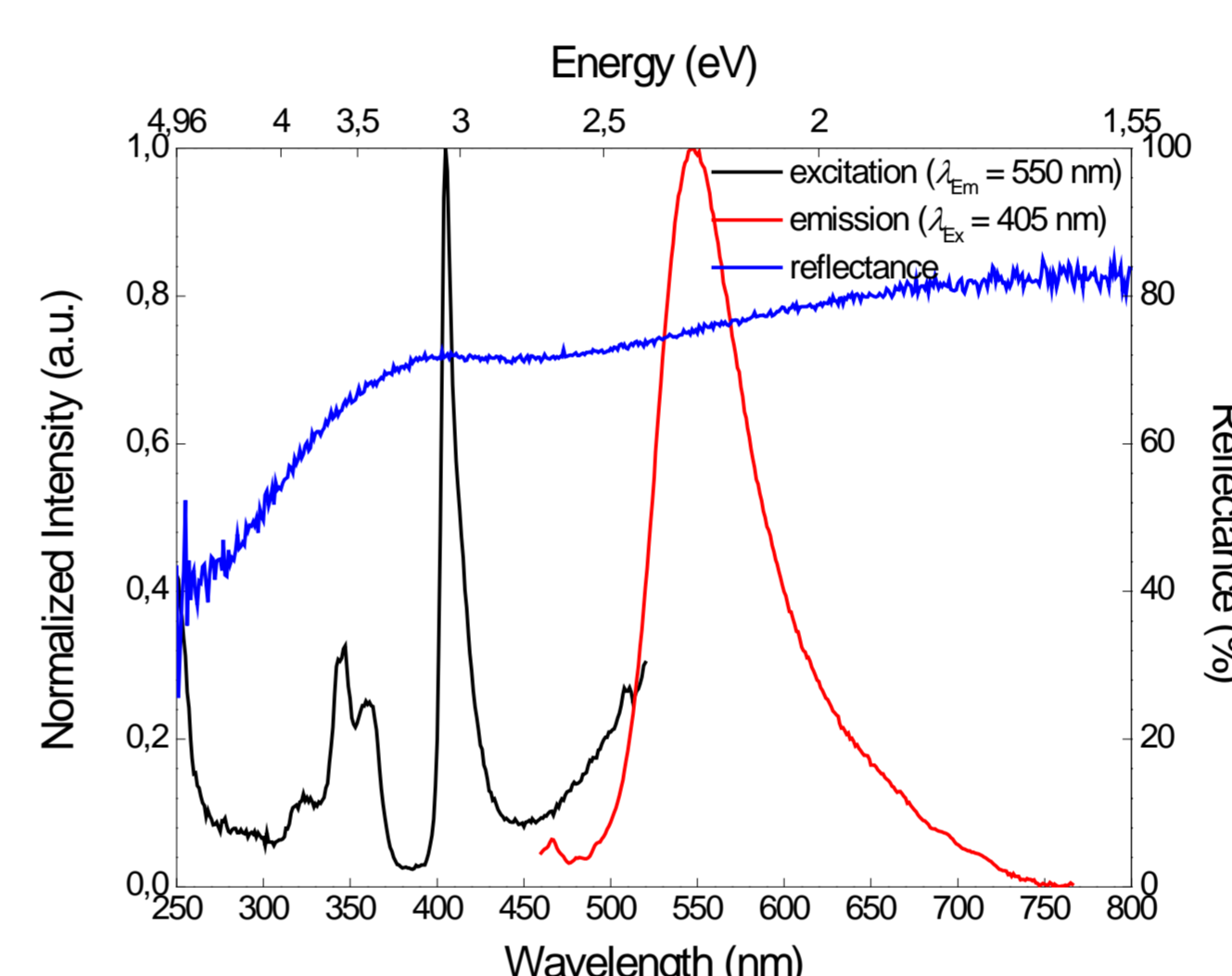


Fig. 4. Excitation, emission and reflectance spectra of Ca_{2.97}Mn_{0.03}Y_{1.98}Ce_{0.02}(Si₃O₉)₂.

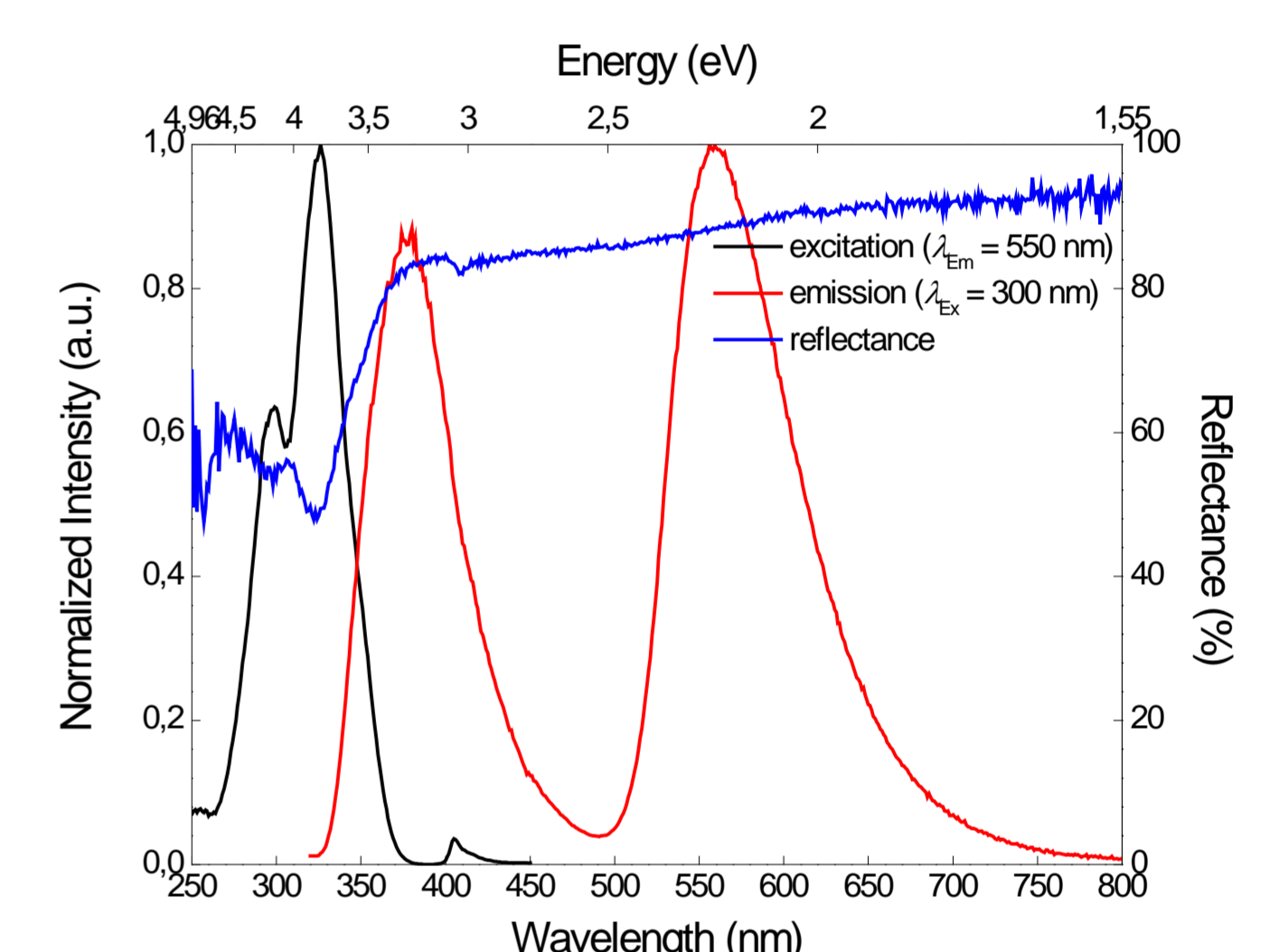


Fig. 5. Excitation, emission and reflectance spectra of Ca_{2.52}Mn_{0.48}Y_{1.98}Ce_{0.02}(Si₃O₉)₂.

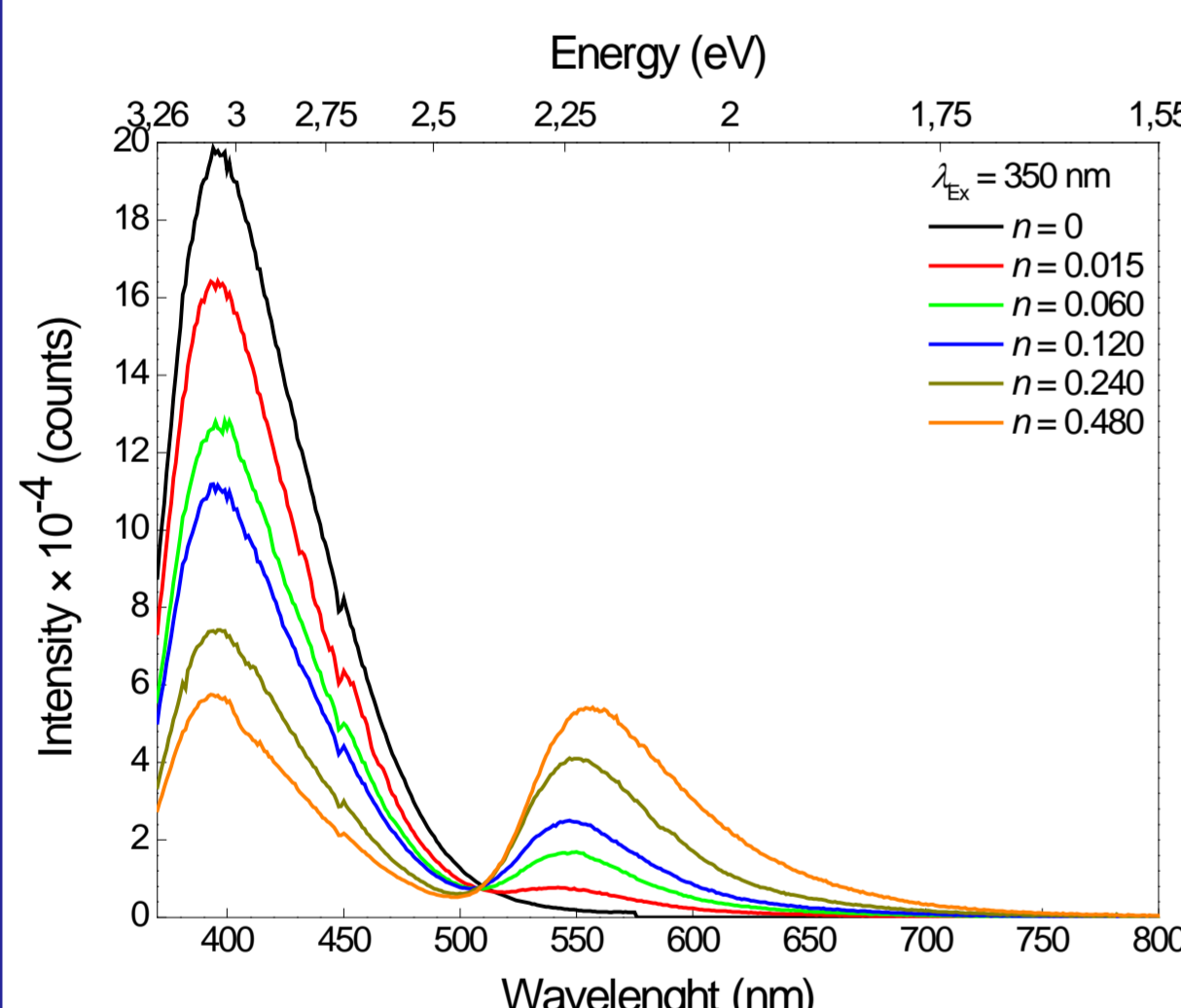


Fig. 6. Emission spectra of Ca₃Y₂(Si₃O₉)₂:Ce³⁺,Mn²⁺ with different Mn²⁺ concentrations.

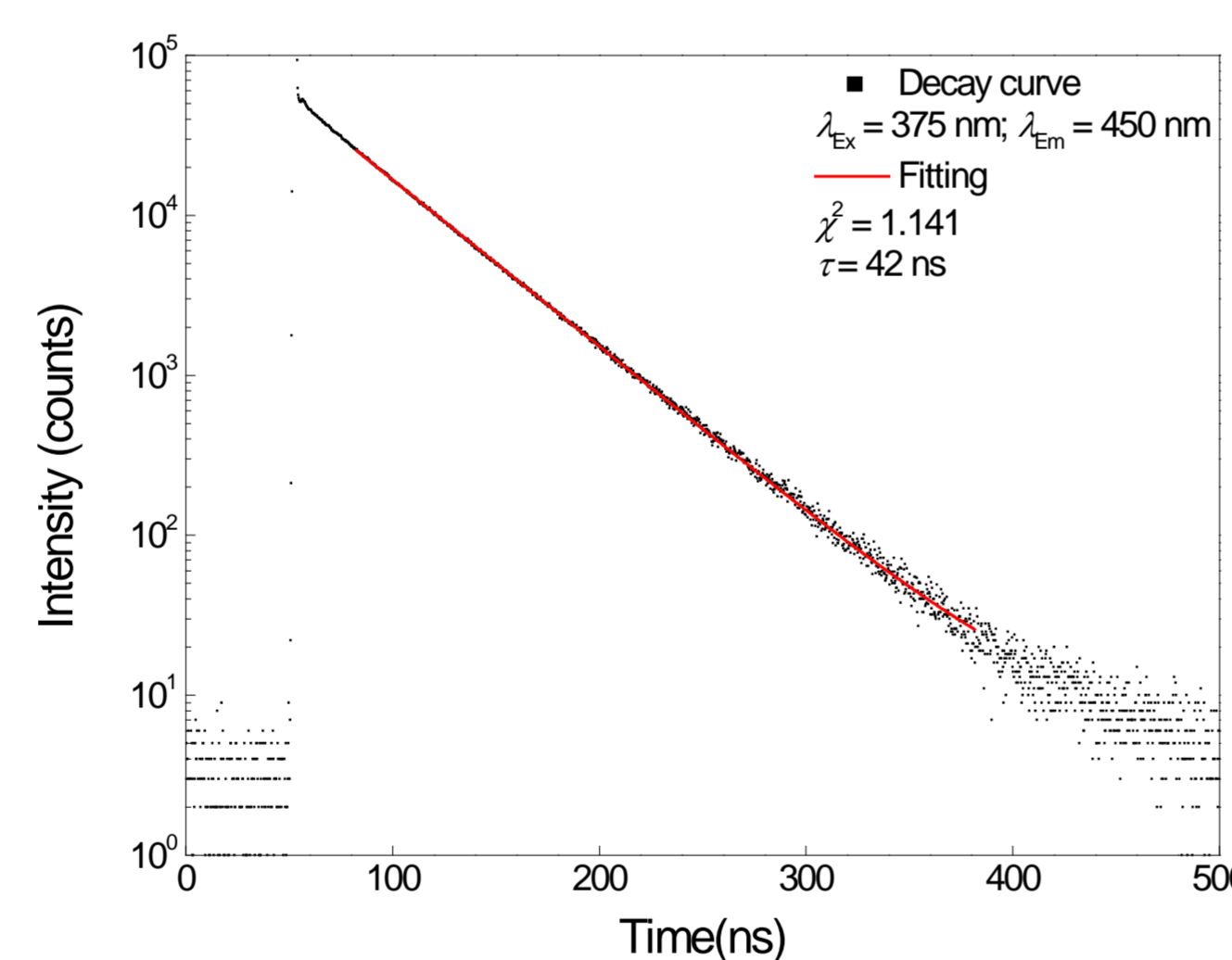


Fig. 7. Decay curve and fitting function of Ca_{2.97}Mn_{0.03}Y_{1.98}Ce_{0.02}(Si₃O₉)₂.

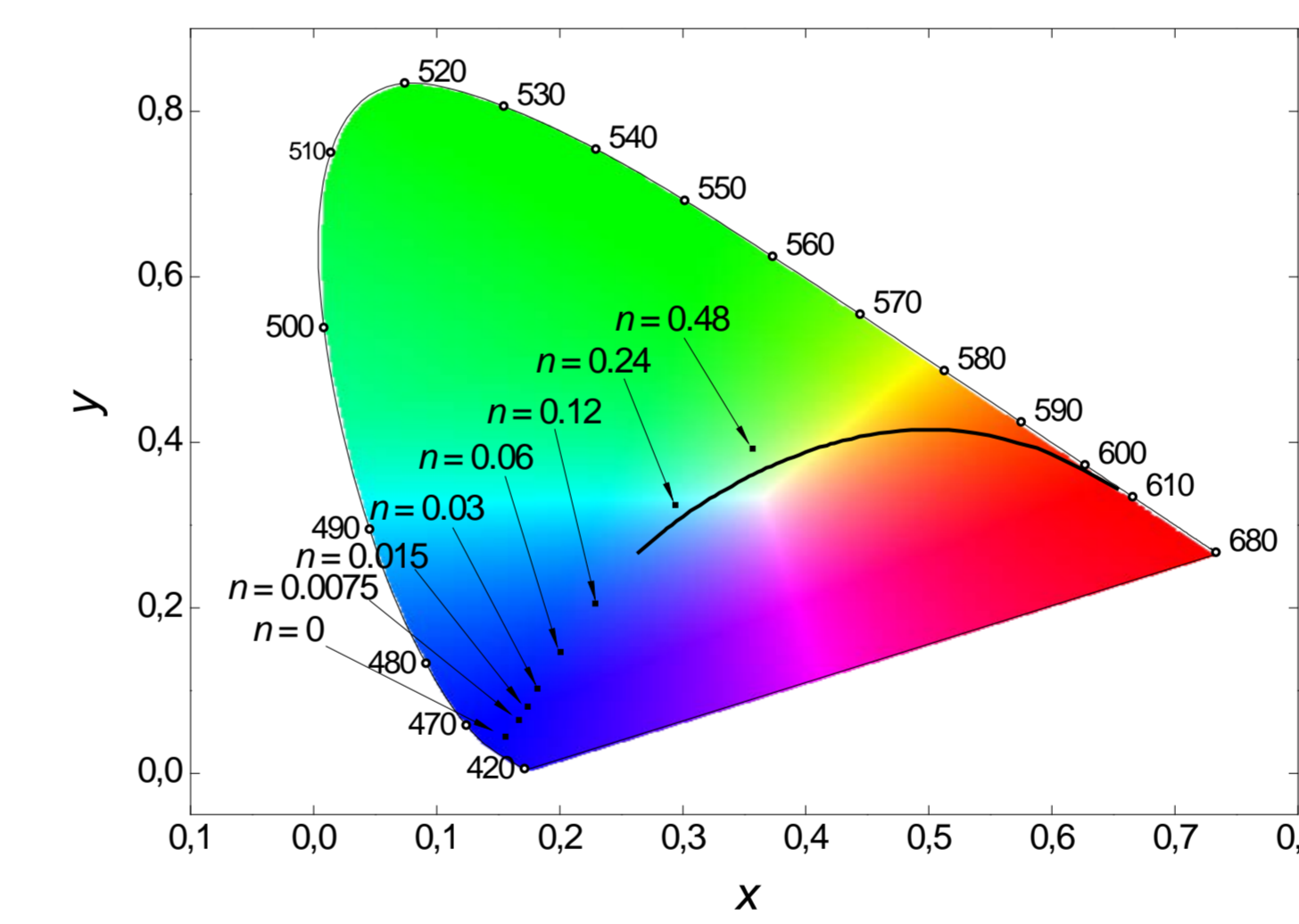


Fig. 8. 1931 CIE chromaticity diagram of Ca₃Y₂(Si₃O₉)₂:Ce³⁺,Mn²⁺.

Table 2
Decay times τ, quantum efficiency QE, luminous equivalent LE and color points of Ca₃Y₂(Si₃O₉)₂:Ce³⁺,Mn²⁺.

Sample (n)	τ (ns)	QE (%)	LE (lm·W ⁻¹)	Color Point (x y)
0	42	75	22	(0.156 0.044)
0.003	43	77	24	(0.161 0.048)
0.0075	42	72	32	(0.167 0.064)
0.015	42	61	41	(0.174 0.080)
0.03	42	71	52	(0.182 0.102)
0.06	42	59	79	(0.201 0.146)
0.12	41	59	117	(0.229 0.205)
0.24	39	49	212	(0.294 0.324)
0.48	37	62	279	(0.357 0.392)

Discussion

- As shown in Figure 2 X-ray diffraction patterns of the as-synthesized Ca₃Y₂(Si₃O₉)₂:Ce³⁺,Mn²⁺ samples with various doping concentrations fit well to the ICDD reference card and show the monoclinic Ca₃Y₂(Si₃O₉)₂ phase.
- Luminescence and reflectance spectra of Ca₃Y_{1.98}Ce_{0.02}(Si₃O₉)₂ are depicted in Figure 3. The excitation spectrum of Ca₃Y_{1.98}Ce_{0.02}(Si₃O₉)₂ consists of various bands due to the 5d¹ multiplets of the Ce³⁺ excited states. The emission spectrum shows a broad band peaking at 380 nm with a tail on the long-wavelength side due to the spin-orbit splitting of the Ce³⁺ ground state (²F_{7/2} and ²F_{5/2}). The reflectance spectrum shows high reflectance in the visible range of light and therefore Ca₃Y_{1.98}Ce_{0.02}(Si₃O₉)₂ exhibits a white body color.
- Luminescence and reflectance spectra of Ca_{2.97}Mn_{0.03}Y_{1.98}Ce_{0.02}(Si₃O₉)₂ are depicted in Figure 4. The excitation spectrum shows four bands at 324, 345, 360 and 405 nm which can be assigned to transitions from the ⁶A₁(⁶S) ground state to the ⁴T₁(⁴P), ⁴E(⁴D), ⁴T₂(⁴D) and [⁴E(⁴G), ⁴A₁(⁴G)] excited states. The emission spectrum shows a broad band with a maximum at 548 nm due to the spin- and parity-forbidden ⁴T₁(⁴G)→⁶A₁(⁶S) transition. The Ca_{2.97}Mn_{0.03}Y_{1.98}Ce_{0.02}(Si₃O₉)₂ exhibits a slightly brownish body color due to the absorption in the visible range of light.
- Figure 5 shows the luminescence and reflectance spectra of Ca_{2.52}Mn_{0.48}Y_{1.98}Ce_{0.02}(Si₃O₉)₂. The excitation spectrum of Ca_{2.52}Mn_{0.48}Y_{1.98}Ce_{0.02}(Si₃O₉)₂ shows the ²F_{7/2}, ²F_{5/2}→5d¹ excitation of Ce³⁺ as well as the ⁶A₁(⁶S)→[⁴E(⁴G), ⁴A₁(⁴G)] excitation of Mn²⁺. Since the excitation spectrum was recorded for the Mn²⁺ emission the observed Ce³⁺ excitation is an indication for the energy transfer from Ce³⁺ to Mn²⁺.
- Figure 6 shows the emission spectra of Ca₃Y₂(Si₃O₉)₂:Ce³⁺,Mn²⁺ with different Mn²⁺ concentrations. The emission intensity of Ce³⁺ was found to decrease with increasing Mn²⁺ content. The Mn²⁺ emission increases with increasing Mn²⁺ content. Concentration quenching was not found in the examined samples.
- The decay curve and its fitting function of Ca_{2.97}Mn_{0.03}Y_{1.98}Ce_{0.02}(Si₃O₉)₂ is depicted in Figure 7. Its shape is representative for all codoped Ca₃Y₂(Si₃O₉)₂:Ce³⁺,Mn²⁺ samples. The corresponding decay times can be best fitted with a first-order exponential function. The determined decay times are summarized in Table 2.
- To visualize the color hue chromaticity coordinates were calculated and mapped onto a 1931 CIE chromaticity diagram as it can be seen in Figure 8 and onto Table 2. The chromaticity coordinates range from (0.156|0.044) to (0.357|0.392) and indicate that the color hue is tunable from deep blue to green.
- Furthermore quantum efficiencies QE as well as luminous equivalents LE were calculated. The results are summarized in Table 2. The quantum efficiencies QE decrease with increasing Mn²⁺ content which indicates a decrease in sample quality with increasing Mn²⁺ content. The luminous equivalents increase with increasing Mn²⁺ content due to an increasing fraction of green emission.